CHEMISTRY
A EUROPEAN JOURNAL

DOI: 10.1002/chem.200701478

# Anchoring of Histidine-Tagged Proteins to Molecular Printboards: Self-assembly, Thermodynamic Modeling, and Patterning

**Manon J. W. Ludden,[a] Alart Mulder,[b] Katrin Schulze,[b] Vinod Subramaniam,[c] Robert Tampé,*[b] and Jurriaan Huskens*[a]**

*Dedicated to Professor David N. Reinhoudt on the occasion of his 65th birthday*

**Abstract:** In this paper the multivalent binding of hexahistidine ($His_6$)-tagged proteins to β-cyclodextrin (β-CD) self-assembled monolayers (SAMs) by using the nickel(II) complex of a hetero-divalent orthogonal adamantyl nitrilotriacetate linker (**4**) is described. Nonspecific interactions were suppressed by using monovalent adamantyl-hexa(ethylene glycol) derivative **3**. With the mono-$His_6$-tagged maltose binding protein ($His_6$-MBP), thermodynamic modeling based on surface plasmon resonance (SPR) titration data showed that the MBP molecules in solution were linked, on average, to Ni·**4** in 1:1 stoichiometry. On the surface, however, the majority of $His_6$-MBP was complexed to surface-immobilized β-CDs through three Ni·**4** complexes. This difference is explained by the high effective β-CD concentration at the surface and is a new example of supramolecular interfacial expression. In a similar adsorption scheme, SPR proved that the α-proteasome could be attached to β-CD SAMs in a specific manner. Patterning through microcontact printing of $(His_6)_4$-DsRed-fluorescent timer (DsRed-FT), which is a tetrameric, visible autofluorescent protein, was carried out in the presence of Ni·**4**. Fluorescence measurements showed that the $(His_6)_4$-DsRed-FT is bound strongly through Ni·**4** to the molecular printboard.

**Keywords:** cyclodextrins · host-guest systems · multivalent systems · proteins · self-assembly

## Introduction

Proteins can be immobilized at surfaces by covalent immobilization or physisorption,[1,2] but these methods leave little room for control over the adsorption process. Control over the immobilization of proteins can be reached, however, through supramolecular chemistry.[3–5] Considerable flexibility over protein immobilization can be achieved through the insertion, by bioengineering, of a hexahistidine ($His_6$)-tag into a protein. These His tags can bind to nickel nitrilotriacetate (NiNTA) self-assembled monolayers (SAMs). In this manner, one can control many factors, such as thermodynamics, orientation, and function.[6–8]

Originally, the NiNTA-$His_6$ tag system was developed for the affinity purification of proteins.[9] Nowadays, the technology is increasingly applied to the immobilization of His-tagged proteins on surfaces.[10–20] Multivalence, which is the simultaneous interaction between multiple functionalities on one entity and multiple complementary functionalities on another entity,[21] is an important concept underlying this type of surface immobilization.[10,22–24]

When His-tagged proteins are immobilized on NiNTA SAMs, it is possible to reverse the immobilization by the addition of EDTA or imidazole.[7,25–27] Also, control over the orientation of His-tagged proteins is possible.[11,23,26,28–30] A typical example in this respect is the oriented immobilization of the 20S proteasome on NiNTA SAMs on gold.[31]

[a] Dr. M. J. W. Ludden, Prof. Dr. J. Huskens
Molecular Nanofabrication Group
MESA+ Institute for Nanotechnology
University of Twente, P.O. Box 217
7500 AE Enschede (The Netherlands)
Fax: (+31) 53-489-4645
E-mail: j.huskens@utwente.nl

[b] Dr. A. Mulder, K. Schulze, Prof. Dr. R. Tampé
Institut für Biochemie, Biozentrum Frankfurt
Johann-Wolfgang-Goethe-Universität
Marie-Curie-Strasse 9, 60438 Frankfurt am Main (Germany)
Fax: (+49) 69-798-29495
E-mail: tampe@em.uni-frankfurt.de

[c] Prof. Dr. V. Subramaniam
Biophysical Engineering Group, University of Twente
P.O. Box 217, 7500 AE Enschede (The Netherlands)

Supporting information for this article is available on the WWW under http://www.chemeurj.org/ or from the author.

The 20S proteasome is a large protein complex that is responsible for the degradation of misfolded proteins. It can be His-tagged either at the α or β subunits. When immobilizing the 20S proteasome onto NiNTA SAMs, this results in an end-on (α) or side-on (β) orientation. Through α immobilization of the 20S proteasome it was possible to elucidate the substrate-association step of the protein degradation mechanism.[23]

β-Cyclodextrin (β-CD) is a well-known host for various small hydrophobic organic molecules in aqueous environments.[32] We have modified β-CD with seven heptathioether chains[33,34] to obtain self-assembled monolayers (SAMs) on gold. Such SAMs are ordered and densely packed and have been extensively characterized.[33,34] The binding constants for the binding of monovalent guest molecules to a single β-CD cavity of these SAMs are comparable to the binding constants for the binding of the corresponding molecules to β-CD in solution.[32,34] All guest binding sites in the β-CD SAM are equivalent and independent, and thus, the β-CD monolayer can be regarded as a multivalent CD host surface. The use of multivalent[35,36] host–guest interactions allows the formation of kinetically stable assemblies, and thus, local complex formation, for example, by patterning, so that these surfaces can be viewed as "molecular printboards".[37,38] By varying the number and type of guest sites, it is possible to control the thermodynamics, kinetics, and stoichiometry of the adsorption and desorption of multivalent molecules at such surfaces.[39]

The enhancement of the adsorption of a multivalent species at the β-CD molecular printboard was previously demonstrated by surface plasmon resonance (SPR) titration experiments in which a heterotropic,[40,41] orthogonal motif was used.[42] In that study, an adamantyl-functionalized ethylenediamine ligand complexed to $M^{II}$ (M is Cu or Ni) was assembled at the surface.[42] In solution, the metal–ligand complex was mostly monovalent. At the surface, however, a multivalent complex was formed. The formation of multivalent complexes at the β-CD molecular printboard is governed by a high effective concentration ($C_{eff}$), which represents the probability of a guest site of an already partially bound multivalent guest moiety finding a complementary host site at a multivalent host (here the printboard).[35,36,39] This $C_{eff}$ results in an increased stability of multivalent complexes at the molecular printboard relative to monovalent complexes. Enhancement factors of $\approx 100$ for the formation of a multivalent complex at the surface compared with in solution were observed.

The versatility of the molecular printboard for attaching proteins was demonstrated in studies in which streptavidin was linked to the molecular printboard in a specific manner through orthogonal linkers.[22] Nonspecific interactions of proteins with those surfaces can be inhibited with a specifically developed adamantyl-functionalized oligo(ethylene glycol) derivative.[43]

In this paper, the advantages of protein attachment to the molecular printboard, for example, controllable binding constants ($K_a$) and the suppression of nonspecific interactions, are combined with His-tagged proteins. The $His_6$-tagged proteins are immobilized on β-CD SAMs by an adamantyl-NTA (**4**) linker. Titration experiments with the maltose binding protein (MBP) that contains a single $His_6$ tag are described, as well as the modeling of these experiments in which the valence of the complex formation in solution and at the surface is compared. The possibility of patterning proteins with multiple His tags is demonstrated by using $(His_6)_4$-DsRed-FT, a variant of the tetrameric reef coral, the visible, autofluorescent protein DsRed. For the α-His-tagged 20S proteasome, the possibility of specific immobilization is discussed.

## Results and Discussion

**Systems under study**: The compounds used in this study are depicted in Scheme 1. The two adamantyl-bearing molecules (**3** and **4**) were developed for the specific attachment of His-tagged proteins to β-CD SAMs (**2**). The adamantyl moiety of **3** and **4** ensures interaction with the β-CD SAM, whereas the hexa(ethylene glycol) (HEG) chain of **3** prevents nonspecific protein adsorption.[43] The NTA moiety of **4**, when complexed to nickel, ensures a specific interaction with $His_6$-tagged proteins.

In this work, three different proteins of varying size and different numbers of $His_6$ tags have been studied: The maltose binding protein (MBP), the fluorescent timer mutant of DsRed (DsRed-FT), and 20S proteasome (Scheme 1). MBP is a protein with a molecular weight of 41 kDa ($3\times4\times6.5$ nm),[44] which is part of the maltose/maltodextrin system of *Escherichia coli* that is responsible for the uptake and efficient metabolism of maltodextrins.[45] The version employed here bears one $His_6$ tag. The $His_6$ tag spans $\approx 2$ nm and the β-CD cavities are spaced at about 2.1 nm from each other, which means that the Ni·**4** complexes bound to the $His_6$ tag are spaced far enough apart to form multiple host–guest complexes at the β-CD surface. Considering the size of the protein and the surface area of the surface-confined β-CD cavities, it should be noted that the MBP is somewhat larger than three β-CD cavities, which corresponds to the maximum number of linkers (**4**) through which $His_6$-MBP can be bound. Therefore, a close-packed layer of protein is expected.

The experiments presented herein were performed at pH 7.5. At this pH, the Ni·**4** complex is formed $>90\,\%$ when $[Ni]_{tot} = [\mathbf{4}]_{tot} > 50$ nM, which is true for every data point shown. In the modeling studies (shown below) it is therefore assumed that Ni·**4** is always completely formed.[46,47]

The fluorescent timer mutant of DsRed (DsRed-FT) is an autofluorescent, tetrameric protein[48–51] and into each monomer a $His_6$ tag was inserted through bioengineering. When this protein is attached to a surface, at least two $His_6$ tags will be facing the surface, and possibly as many as three or four, as a result of the deformation of the tertiary or quaternary structure of the protein. The fluorescent properties of this protein are sensitive to changes in the tertiary structure

  

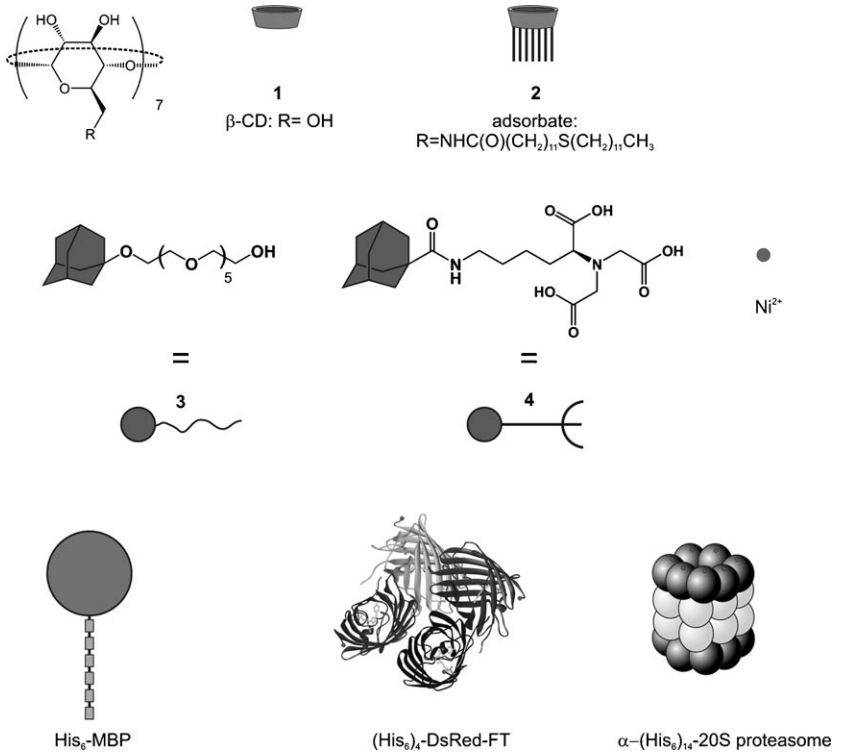


Scheme 1. Compounds used in this study: β-cyclodextrin (**1**), adsorbate for SAMs on gold (**2**), adamantyl linkers **3** and **4**, nickel, $His_6$-MBP, $(His_6)_4$-DsRed-FT, and α-$(His_6)_{14}$-20S proteasome.

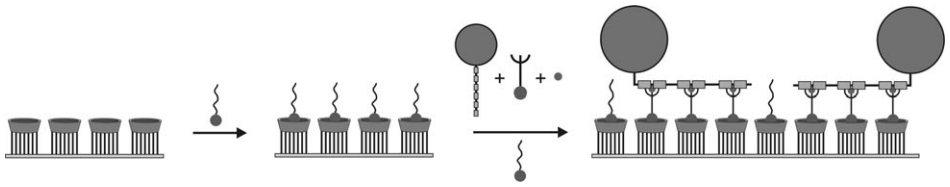

Scheme 2. Binding of $His_6$-MBP through Ni·**4** to β-CD SAMs, in competition with monovalent blocking agent **3**.

and the protein may lose its fluorescent properties upon large conformational changes.

20S proteasome is a large protein complex (700 kDa) that consists of two different subunits (α and β, 14 of each) with a high homology. The size of the protein is about 15 nm in height and 10 nm in diameter, which means that, if 20S proteasome is immobilized end-on (α form) on the molecular printboard, it spans about 20 β-CD cavities. The two outer rings consist of seven α subunits, whereas the two inner rings consist of seven β subunits. In the proteasome employed herein, the $His_6$ tags are inserted into the α subunits. Binding to the surface is therefore expected to be through 7 $His_6$ tags, and thus, 21 NTA linkers bound to 21 β-CD cavities, which fits well with the cross-section of the proteasome.[23]

**Binding of the mono-His-tagged MBP**: The immobilization of His-tagged proteins on β-CD SAMs through Ni·**4** was first studied by SPR titration experiments with $His_6$-MBP. The assembly scheme is schematically shown in Scheme 2. Figure 1 shows the corresponding SPR titration curve.

The SPR titration experiment was performed by monitoring additions of increasing concentrations of $His_6$-MBP and Ni·**4** against a background of **3** (0.1 mM) in phosphate-buffered saline (PBS). This concentration suffices to inhibit the non-specific interactions of proteins with the β-CD SAM.[43] Throughout this study the His tag/Ni·**4** ratio was kept at 1:5, that is, a two equivalent excess over the three equivalents that are maximally expected to interact with a His tag. After each addition, an increase in the SPR signal was observed, which is indicative of adsorption (Figure 1). The adsorption was followed for 10 min, after which the surface was regenerated by using β-CD (10 mM) and EDTA (10 mM), which led to restoration of the baseline and indicated desorption of the $His_6$-MBP complex from the surface. Figure 1 shows a steady increase in the baseline. This is attributed to drift because

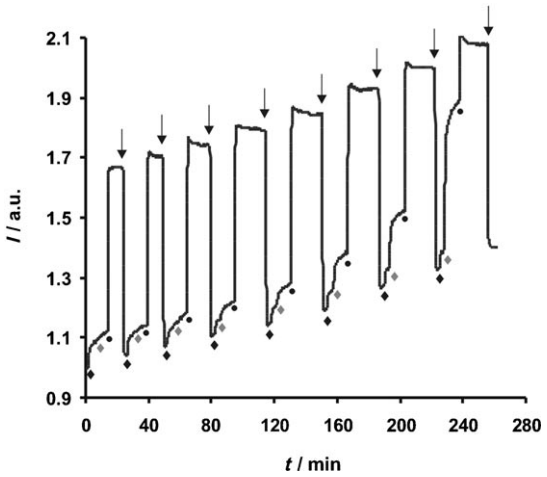


Figure 1. SPR sensogram of a titration experiment of $His_6$-MBP with the molecular printboard (Scheme 2). Symbols indicate switching to: 0.1 mM **3** in PBS (♦), increasing concentrations of $His_6$-MBP + Ni·**4** (ratio 1:5) + 0.1 mM **3** in PBS (◆), 10 mM β-CD + 10 mM EDTA in PBS (●), PBS (↓).

  

every addition of **3** before the addition of $His_6$-MBP and Ni·**4** resulted in a similar increase in the SPR signal. Furthermore, each addition, with an increasing concentration of $His_6$-MBP, resulted in a greater increase in the SPR signal. The equilibrium adsorption SPR values were plotted against the concentration of $His_6$-MBP (Figure 2).

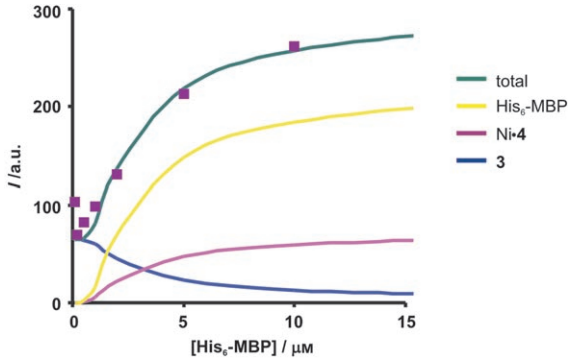


Figure 2. Equilibrium values of the SPR intensities (■) of the titration shown in Figure 1 and corresponding fit to the model and contributions by different components to the signal (solid lines).

The data points generated by the SPR titration experiment, shown in Figure 2, were fitted by using a model that accounts for the interaction of **3** and Ni·**4** with β-CD in solution (β-$CD_l$) and with the β-CD SAM (β-$CD_s$), as well as the interaction of Ni·**4** with $His_6$-MBP. A complete description of this model can be found in the Supporting Information. From isothermal titration calorimetry (ITC) measurements, the binding constants ($K_a$) for **4** and **3** with β-$CD_l$ were determined to be $K_a=(6.6\pm0.3)\times10^4$ and $(5.5\pm1.3)\times10^4\,M^{-1}$, respectively.[43] These are typical binding constants for monovalent β-CD–adamantyl interactions.[32] The complexation binding constants for the interaction of **3** and Ni·**4** with β-$CD_s$ were determined by SPR titrations. Fitting of the data led to $K_a$ values of $(2.6\pm0.9)\times10^4$ and $(1.2\pm0.2)\times10^4\,M^{-1}$ for **3**·β-$CD_s$ and **4**·β-$CD_s$, respectively. These binding constants are comparable to those found in solution and are also typical of monovalent β-CD–adamantyl interactions.

The main fitting parameter used in the model was the value of the first interaction of additional Ni·**4** units binding to the $His_6$ tag ($K_1$). The second ($K_2$) and third ($K_3$) binding constants for additional Ni·**4** units binding to the $His_6$ tag are linked to $K_1$ by statistical factors, that is, $^6/_{25}$ and $^7/_{225}$, respectively (see the Supporting Information). Fitting of the curve in Figure 2 resulted in $K_1=7.8\times10^4\,M^{-1}$, and thus, $K_2=1.9\times10^4$ and $K_3=2.4\times10^3\,M^{-1}$. These are close to the binding constants found in the literature.[52]

The modeled data presented in Figure 2 show that the concentrations of $His_6$-MBP and **4** at the surface increase and that the concentration of **3** decreases, in agreement with the expected competition. This competition is efficient because the complex of $His_6$-MBP bound to Ni·**4** at β-CD SAMs is multivalent and governed by $C_{eff}$, which is stronger than the monovalent binding of **3**. The total SPR signal is the sum of the intensity change of the three different components ($His_6$-MBP, **3**, Ni·**4**). With the equilibria shown in Scheme 2 (see the Supporting Information) and the binding constants obtained for **3** and **4** in solution and at the surface, it is possible to determine the speciation in both phases. Figure 3 shows the speciation of all of the MBP species bound to $x$ Ni·**4** complexes ($x=0$–3) in solution and at the surface. Thus, the valence of the MBP complexes can be determined.

From the modeled data presented in Figure 3 several observations can be made. At sub-μM concentrations, there is almost no interaction between $His_6$-MBP and Ni·**4** in solution. At higher concentrations the majority of $His_6$-MBP is complexed in a monovalent fashion to Ni·**4**. A smaller fraction is bound to two Ni·**4** moieties and there is hardly any $His_6$-MBP present that is bound to three NiNTA moieties. At the surface, however, the situation is completely different. At low concentrations, the occupation of the molecular printboard with $His_6$-MBP is still low, which occurs as a result of the way in which the experiments were performed, that is, the concentrations of both $His_6$-MBP and Ni·**4** increase simultaneously. Nevertheless, the valence of binding of $His_6$-MBP to the molecular printboard is already divalent for about 60% of $His_6$-MBP with 20% of $His_6$-MBP bound in a trivalent fashion. Above 0.15 μM, the concentration of surface-immobilized $His_6$-MBP increases rapidly, and this increase can be almost completely attributed to trivalently bound $His_6$-MBP. Above 1 μM, the majority (≈85%) of $His_6$-MBP is bound in a trivalent fashion to the molecular printboard, whereas a smaller fraction (≈15%) is bound in a divalent fashion. The amount of monovalently bound $His_6$-MBP is negligible.

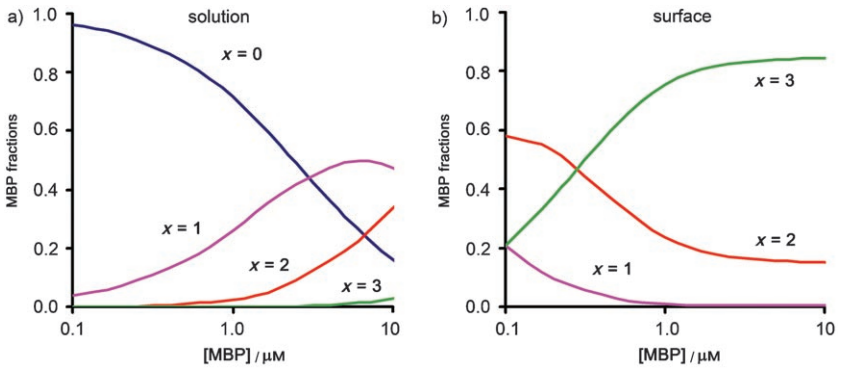


Figure 3. Thermodynamic data modeling showing fractions of $His_6$-MBP·(Ni·**4**)$_x$ (i.e., complexed to different numbers, $x$, of Ni·**4**) as a function of [$His_6$-MBP] a) in solution and b) at the surface.

  

The surface multivalence enhancement observed here resembles the surface enhancement of a coordination complex observed previously and can be ascribed to the high effective concentration at the surface promoting multivalent binding.[42] The enhancement can be expressed by an enhancement factor (*EF*) that can be calculated according to Equation (1), in which $f$ is the fraction of MBP in solution (l) or at the surface (s) bound in a mono- or multivalent fashion to Ni·**4**.

$$EF_{\text{multi}} = \frac{f_{\text{s,multi}}/f_{\text{s,mono}}}{f_{\text{l,multi}}/f_{\text{l,mono}}} \quad (1)$$

Figure 4 shows the calculated enhancement factors as a function of concentration. At low concentrations the enhancement factor for divalent binding to the printboard is 300, and decreases at higher concentrations. For the trivalent species, the surface multivalence effect is considerably larger. The $EF_{\text{tri}}$ value is close to $10^4$ at low concentrations and also decreases gradually. It can therefore be concluded that the multivalent β-CD host surface favors the formation of multivalent complexes and that this effect is stronger for complexes with a higher valence.

**Adsorption of 20S proteasome at the molecular printboard**: Nonspecific interactions of 20S proteasome with β-CD SAMs were investigated by SPR. As control over protein orientation at the surface is the final goal, α-His-tagged 20S proteasome was used to target an end-on immobilization. SPR titration experiments with 20S proteasome performed as described above for $His_6$-MBP indicated that a 0.1 M solution of **3** was insufficient for complete inhibition of nonspecific interactions. Typical SPR sensograms obtained with 20S proteasome are shown in Figure 5.

In Figure 5a, SPR sensograms are depicted that show that 20S proteasome adsorbs nonspecifically at the β-CD SAM in the absence of **3**. Addition of 0.5 and 1 mM **3** to the PBS buffer reduced the amount of nonspecific adsorption by 36 and 62%, respectively. Experiments in which Ni·**4** was used were performed to check if 20S proteasome could be immobilized in a specific manner in the presence of **3** (Figure 5b). Therefore, 20S proteasome was premixed with Ni·**4** (ratio 1:70) and **3** (1 mM) before the SPR experiments were performed. Thereafter, this mixture was passed over the β-CD SAM. The increase in the SPR signal was much higher in this case, indicating that 20S proteasome is immobilized to a large extent in a specific manner through **4**. The rapid decrease in the SPR signal after switching to **3** (1 mM) in PBS is remarkable as it indicates labile binding. Theoretically, 20S proteasome would be expected to be attached to the β-CD SAMs in a strong multivalent fashion to give a complex that is stable against rinsing with PBS. Possibly the position of the $His_6$ tag in combination with the length of linker **4** does not allow a high valence to be achieved. This will be investigated in another study by varying the linker length of linker **4**.

**Patterning of DsRed-FT at the molecular printboard**: Patterning experiments were performed with tetravalent $(His_6)_4$-DsRed-FT. Surface-patterning by microcontact printing was performed with oxidized poly(dimethylsiloxane) (PDMS) stamps. These stamps were inked for 2 min with a solution that contained $(His_6)_4$-DsRed-FT ($1\times10^{-6}$ M) and

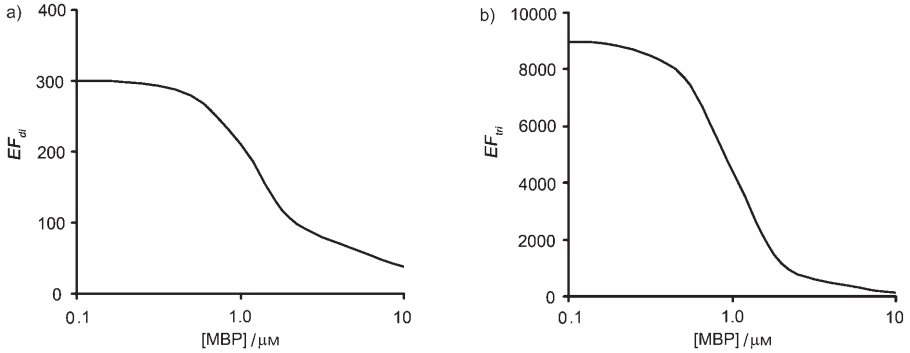


Figure 4. Enhancement factors (*EF*) for a) the divalent and b) the trivalent species present at the β-CD SAMs measured relative to the corresponding solution species.

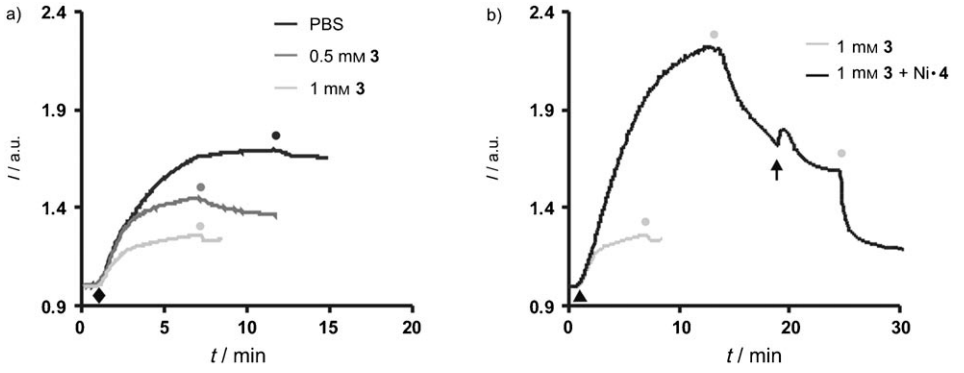


Figure 5. a) SPR sensograms of the nonspecific adsorption, and the inhibition thereof, of the α-$(His_6)_{14}$-20S proteasome onto β-CD SAMs in the absence and presence of **3** (1 mM). b) SPR sensograms of the specific adsorption of the α-$(His_6)_{14}$-20S proteasome (0.1 μM) onto β-CD SAMs in the presence of **3** (1 mM) and in the absence and presence of Ni·**4** (7 μM). Symbols indicate switching solutions to: PBS (●); 0.5 mM **3** in PBS (●); 1.0 mM **3** in PBS (●); 0.1 μM 20 S proteasome in PBS, 0.5 mM **3** in PBS and 0, 0.5, or 1.0 mM **3** in PBS (◆); 0.1 μM 20S proteasome, 7 μM Ni·**4** in PBS, and 1 mM **3** (▲); 10 mM β-CD and 10 mM EDTA in PBS (↑).

  

Ni·**4** ($2\times10^{-6}$ M) in PBS buffer. After inking, the stamp was blown dry and put into conformal contact with a β-CD SAM on glass for 1 min.[53] After printing, the sample was imaged by fluorescence microscopy (Figure 6, top). A reference experiment was performed in which the oxidized stamp was inked with $1\times10^{-6}$ M $(His_6)_4$-DsRed-FT without Ni·**4** (Figure 6, bottom).

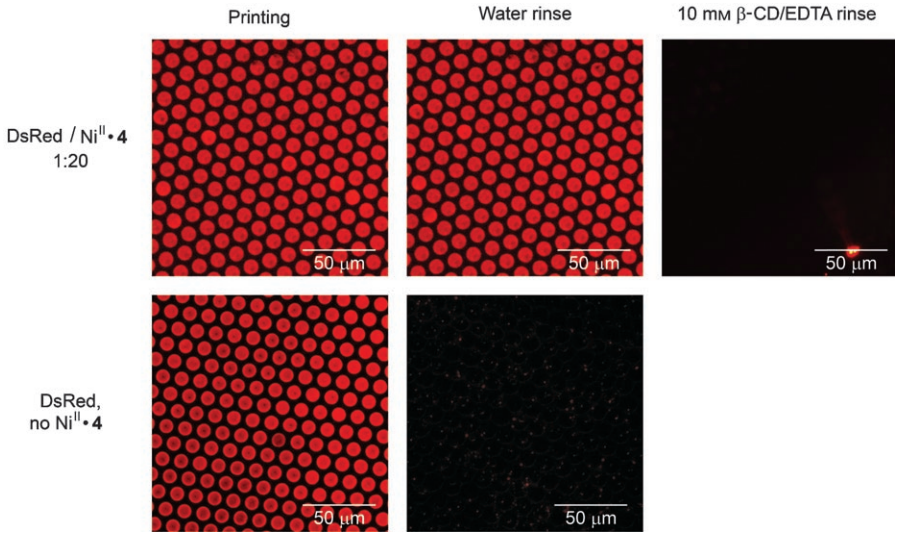


Figure 6. Fluorescence microscopy images of $(His_6)_4$-DsRed-FT at β-CD SAMs patterned by microcontact printing with (top) and without Ni·**4** (bottom), directly after printing (left), rinsing with water (center), and subsequent rinsing with 10 mM β-CD and 10 mM EDTA (right).

After printing, patterns were clearly visible both with and without Ni·**4** which indicates 1) that attachment to the molecular printboard did not disrupt the tertiary structure of the protein and 2) that transfer occurred regardless of the specificity of the interaction. For the sample prepared with Ni·**4** present in the inking solution, rinsing with water did not remove the pattern from the surface, only prolonged rinsing with a PBS solution containing β-CD (10 mM) and EDTA (10 M) appeared to be sufficient for removing $(His_6)_4$-DsRed-FT from the surface. This indicates that complex stability is governed by specific, multivalent interactions. In contrast, the surface patterned with the inking solution that did not contain Ni·**4** could be cleared of $(His_6)_4$-DsRed-FT simply by rinsing with water, which indicates that the protein was not attached in a specific manner.

The number of His tags anchoring the $(His_6)_4$-DsRed-FT protein to the surface remains an open issue. Mathematically speaking, estimating the thermodynamic binding strength of a protein with multiple His tags is a double-nested multivalent problem: Two His groups are anchored to a single Ni·**4** complex, one to three Ni·**4** complexes can be attached to a single $His_6$ tag (and we show here that the majority bind in a trivalent fashion), and one to four His tags of DsRed-FT can be bound through (mostly) three to twelve Ni·**4** complexes to the β-CD substrate. For a single His tag, the overall stability constant for trivalent binding through Ni·**4** is given by Equation (2) (see the Supporting Information):

$$K = (K_i)^3 K_1 K_2 K_3 C_{\mathrm{eff}}^2 [\mathrm{Ni}\cdot\mathbf{4}]^3 \quad (2)$$

An apparent binding constant is therefore strongly dependent on [Ni·**4**] and can be estimated, based on the data given above, to be approximately $10^5\,\mathrm{M}^{-1}$ when [Ni·**4**] = 1 μM. The stability of the DsRed-FT patterns towards rinsing with water may indicate binding with multiple (2 to 4) His tags, and thus, explain the qualitatively similar behavior that is observed for the binding of a divalent adamantyl derivative.[38,54] However, kinetic effects, that is, slow dissociation and redissociation of the protein, cannot be excluded at this stage. More experimental work, both regarding the thermodynamics and the kinetics of such nested multivalent systems, as well as the thermodynamic modeling of such systems, is needed before firm conclusions can be reached.

## Conclusion

This paper shows that $His_6$-tagged proteins can be attached to a molecular printboard in a selective manner by using the supramolecular blocking agent **3** and Ni·**4**. Modeling of the SPR data of $His_6$-MBP binding to the molecular printboard showed that enhancement of surface multivalence occurs upon binding of $His_6$-MBP to the molecular printboard. Although the binding of $His_6$-MBP to Ni·**4** in solution is mainly absent or monovalent, the binding of $His_6$-MBP to Ni·**4** on the molecular printboard is mainly trivalent. Surface enhancement factors for the divalent species are as high as ≈300 and for the trivalent species up to $10^4$. SPR studies with 20S proteasome showed that nonspecific interactions of the protein with the molecular printboard can be suppressed by up to 62%. Nevertheless the possibility of specific adsorption became apparent in the presence of Ni·**4**, although the final stability appeared to be rather low. Patterning experiments with the autofluorescent protein $(His_6)_4$-DsRed-FT showed that the protein, complexed to Ni·**4**, can be patterned by means of microcontact printing on the molecular printboard in a specific, stable, multivalent manner. This work shows that different layers of noncovalent interactions can lead to a very stable attachment of proteins to surfaces. The research presented here forms a basis from which the

  

attachment of His-tagged proteins to β-CD SAMs can be extended, for example, to the development of protein arrays.

## Experimental Section

**General:** The synthesis of **2**, **3**, **4**, and β-CD heptamine has been previously described.[22,33,43,55] Maltose binding protein (MBP) with a C-terminal hexahistidine tag was expressed and purified as previously described.[8] The α-His-tagged 20S proteasome was expressed and purified as previously described.[23] For all experiments 10 mM phosphate buffer (pH 7.5) with 150 mM NaCl, that is, phosphate-buffered saline (PBS), was used.

**Monolayer preparation**: Gold substrates for SPR (BK7 glass/2–4 nm Ti/50 nm Au) were obtained from Ssens B.V. (Hengelo, The Netherlands). The gold substrates were cleaned by dipping them into piranha solution (1:3 mixture of concentrated $H_2SO_4$ and 30% $H_2O_2$) for 5 s. (**WARNING**: piranha solution should be handled with caution; it can detonate unexpectedly.) After thorough rinsing with millipore water they were placed for 10 min in absolute EtOH to remove the oxide layer. Subsequently, β-CD SAMs of **2** were prepared as described previously.[33] β-CD SAMs on glass were prepared by using β-CD heptamine, as described before.[53] All solvents used in the monolayer preparations were of p.a. grade.

**Surface plasmon resonance:** SPR measurements were performed by using a Resonant Probes SPR instrument. The instrument consists of a HeNe laser (JDS Uniphase, 10 mW, $\lambda = 632.8$ nm) in which the laser light passes through a chopper that is connected to a lock-in amplifier (EG&G 7256). The modulated beam is directed through two polarizers (OWIS) to control the intensity and the plane of polarization of the light. The light is coupled through a high-index prism (Scott, LaSFN9) in the Kretschmann configuration to the backside of the gold-coated substrate which is optically matched through a refractive index matching oil (Cargille; series B; $n_D^{25} = 1.7000 \pm 0.0002$) at the prism, mounted on a $\theta-2\theta$ goniometer, in contact with a Teflon cell with a volume of 39 μL and a diameter of 5 mm. The light that leaves the prism passes through a beam splitter. Subsequently, the s-polarized light is directed to a reference detector and the p-polarized light passes through a lens that focuses the light onto a photodiode detector. Laser fluctuations are filtered out by dividing the intensity of the p-polarized light ($I_p$) by the intensity of the s-polarized light ($I_s$). All measurements were performed at a constant angle by reflectivity tracking.

A Reglo digital MS-4/8 Flow pump from Ismatec with four channels was used. In this flow pump, Tygon R3607 tubing with a diameter of 0.76 mm was used, obtained from Ismatec.

The SPR experiments were performed in a flow cell with a volume of $3.9 \times 10^{-2}$ mL under a continuous flow of 0.5 mL min$^{-1}$. Before an experiment was started, the gold substrates were rinsed thoroughly with 10 mM β-CD in PBS and PBS. Experiments were started after the baseline had stabilized. When the solution had to be changed, the pump was stopped, and immediately after changing the solution the pump was switched on again. Stock solutions ($1 \times 10^{-4}$ M) of the different proteins were prepared in PBS and diluted just before every experiment. In those cases in which protein was used in combination with **4**, the mixture was left to stand for 20 min before use.

**Microcontact printing:** PDMS stamps were prepared by casting a 10:1 (v/v) mixture of poly(dimethylsiloxane) and curing agent (Sylgard 184, Dow Corning) against a patterned silicon master. The master employed had hexagonally oriented 10 μm circular features separated by 5 μm. After curing the stamps overnight, they were mildly oxidized in an oxygen plasma reactor for 30 s to render them hydrophilic. Subsequently they were inked by soaking them in an aqueous solution of $(His_6)_4$-DsRed-FT ($10^{-6}$ M) with or without Ni•**4** ($2 \times 10^{-5}$ M) for 2 min. Before printing the stamps were blown dry in a stream of $N_2$. The stamps were applied manually and without pressure control for 2 min on the β-CD SAMs on gold and then carefully removed.

**Fluorescence microscopy:** Fluorescence microscopy images were made by using an Olympus inverted research microscope IX71 equipped with a mercury burner U-RFL-T as a light source and a Olympus DP70 digital camera ($12.5 \times 10^6$ pixel cooled digital color camera) for image acquisition. Green excitation light ($510 \leq \lambda_{ex} \leq 550$ nm) and red emission light ($\lambda_{em} \geq 590$ nm) was filtered by using a U-MWG Olympus filter cube.

## Acknowledgement

We are grateful for financial support from the Council for Chemical Sciences of the Netherlands Organization for Scientific Research (NWO-CW) (M.J.W.L.; Vidi Vernieuwingsimpuls grant 700.52.423 to J.H.).

[1] A. Biebricher, A. Paul, P. Tinnefeld, A. Gölzhäuser, M. Sauer, *J. Biotechnol.* **2004**, *112*, 97–107.
[2] K. M. McLean, S. L. McArthur, R. C. Chatelier, P. Kingshott, H. J. Griesser, *Colloids Surf., B* **2000**, *17*, 23–35.
[3] A. Fragoso, J. Caballero, E. Almirall, R. Villalonga, R. Caro, *Langmuir* **2002**, *18*, 4467–4471.
[4] G. Y. Liu, N. A. Amro, *Proc. Natl. Acad. Sci. U.S.A.* **2002**, *99*, 5165–5170.
[5] S. A. Miscoria, J. Desbrieres, G. D. Barra, P. Labbé, *Anal. Chim. Acta* **2006**, *578*, 137–144.
[6] R. Valiokas, G. Klenkar, A. Tinazli, R. Tampé, B. Liedberg, J. Piehler, *ChemBioChem* **2006**, *7*, 1325–1329.
[7] E. L. Schmid, T. A. Keller, Z. Dienes, H. Vogel, *Anal. Chem.* **1997**, *69*, 1979–1985.
[8] S. Lata, J. Piehler, *Anal. Chem.* **2005**, *77*, 1096–1105.
[9] J. Porath, J. Carlsson, I. Olsson, G. Belfrage, *Nature* **1975**, *258*, 589–599.
[10] G. Klenkar, R. Valiokas, I. Lundstrom, A. Tinazli, R. Tampé, J. Piehler, B. Liedberg, *Anal. Chem.* **2006**, *78*, 3643–3650.
[11] A. Tinazli, J. L. Tang, R. Valiokas, S. Picuric, S. Lata, J. Piehler, B. Liedberg, R. Tampé, *Chem. Eur. J.* **2005**, *11*, 5249–5259.
[12] R. Gamsjaeger, B. Wimmer, H. Kahr, A. Tinazli, S. Piruric, S. Lata, R. Tampé, Y. Maulet, H. J. Gruber, P. Hinterdorfer, C. Romanin, *Langmuir* **2004**, *20*, 5885–5890.
[13] R. Blankespoor, B. Limoges, B. Schöllhorn, J. L. Sysa-Magalé, D. Yazidi, *Langmuir* **2005**, *21*, 3362–3375.
[14] E. Gizeli, J. Glad, *Anal. Chem.* **2004**, *76*, 3995–4001.
[15] J. K. Lee, Y. G. Kim, Y. S. Chi, W. S. Yun, I. S. Choi, *J. Phys. Chem. B* **2004**, *108*, 7665–7673
[16] K. Kato, H. Sato, H. Iwata, *Langmuir* **2005**, *21*, 7071–7075.
[17] D. Kröger, M. Liley, W. Schiweck, A. Skerra, H. Vogel, *Biosens. Bioelectron.* **1999**, *14*, 155–161.
[18] U. Rädler, J. Mack, N. Persike, G. Jung, R. Tampé, *Biophys. J.* **2000**, *79*, 3144–3152.
[19] L. Schmitt, T. M. Bohanon, S. Denzinger, H. Ringsdorf, R. Tampé, *Angew. Chem.* **2001**, *108*, 344–347; *Angew. Chem. Int. Ed. Engl.* **1996**, *35*, 317–320.
[20] G. J. Wegner, H. J. Lee, G. Marriott, R. M. Corn, *Anal. Chem.* **2003**, *75*, 4740–4746.
[21] M. Mammen, S.-K. Choi, G. M. Whitesides, *Angew. Chem.* **1998**, *110*, 2908–2953; *Angew. Chem. Int. Ed.* **1998**, *37*, 2754–2794.
[22] M. J. W. Ludden, M. Péter, D. N. Reinhoudt, J. Huskens, *Small* **2006**, *2*, 1192–1202.
[23] S. Hutschenreiter, A. Tinazli, K. Model, R. Tampé, *EMBO* **2004**, *23*, 2488–2497.
[24] S. Lata, M. Gavutis, R. Tampé, J. Piehler, *J. Am. Chem. Soc.* **2006**, *128*, 2365–2372.
[25] E. L. Schmid, T. A. Keller, Z. Dienes, H. Vogel, *Anal. Chem.* **1997**, *69*, 1979–1985.
[26] N. Haddour, S. Cosnier, C. Gondran, *J. Am. Chem. Soc.* **2005**, *127*, 5752–5753.

  

[27] G. Zhen, D. Falconnet, E. Kuennemann, J. Vörös, N. D. Spencer, M. Textor, S. Zürcher, *Adv. Funct. Mater.* **2006**, *16*, 243–251.
[28] I. T. Dorn, K. Pawlitschko, S. C. Pettinger, R. Tampé, *Biol. Chem.* **1998**, *379*, 1151–1159.
[29] C. Dietrich, L. Schmitt, R. Tampé, *Proc. Natl. Acad. Sci. U.S.A.* **1995**, *92*, 9014–9018.
[30] A. Thess, S. Hutschenreiter, M. Hofmann, R. Tampé, W. Baumeister, R. Guckenberger, *J. Biol. Chem.* **2002**, *277*, 36321–36328.
[31] I. T. Dorn, R. Eschrich, E. Seemüller, R. Guckenberger, R. Tampé, *J. Mol. Biol.* **1999**, *288*, 1027–1036.
[32] M. V. Rekharsky, Y. Inoue, *Chem. Rev.* **1998**, *98*, 1880–1901.
[33] M. W. J. Beulen, J. Bügler, B. Lammerink, F. A. J. Geurts, E. M. E. F. Biemond, K. G. C. van Leerdam, F. C. J. M. van Veggel, J. F. J. Engbersen, D. N. Reinhoudt, *Langmuir* **1998**, *14*, 6424–6429.
[34] M. W. J. Beulen, J. Bügler, M. R. de Jong, B. Lammerink, J. Huskens, H. Schönherr, G. J. Vancso, B. A. Boukamp, H. Wieder, A. Offenhäuser, W. Knoll, F. C. J. M. van Veggel, D. N. Reinhoudt, *Chem. Eur. J.* **2000**, *6*, 1176–1183.
[35] J. Huskens, A. Mulder, T. Auletta, C. A. Nijhuis, M. J. W. Ludden, D. N. Reinhoudt, *J. Am. Chem. Soc.* **2004**, *126*, 6784–6797.
[36] A. Mulder, T. Auletta, A. Sartori, S. Del Ciotto, A. Casnati, R. Ungaro, J. Huskens, D. N. Reinhoudt, *J. Am. Chem. Soc.* **2004**, *126*, 6627–6636.
[37] J. Huskens, M. A. Deij, D. N. Reinhoudt, *Angew. Chem.* **2002**, *114*, 4647–4651; *Angew. Chem. Int. Ed.* **2002**, *41*, 4467–4471.
[38] T. Auletta, B. Dordi, A. Mulder, A. Sartori, S. Onclin, C. M. Bruinink, M. Péter, C. A. Nijhuis, H. Beijleveld, H. Schönherr, G. J. Vancso, A. Casnati, R. Ungaro, B. J. Ravoo, J. Huskens, D. N. Reinhoudt, *Angew. Chem.* **2004**, *116*, 373–377; *Angew. Chem. Int. Ed.* **2004**, *43*, 369–373.
[39] M. J. W. Ludden, D. N. Reinhoudt, J. Huskens, *Chem. Soc. Rev.* **2006**, *35*, 1122–1134.
[40] M. C. T. Fyfe, J. F. Stoddart, *Coord. Chem. Rev.* **1999**, *183*, 139–155.
[41] H. Hofmeier, U. S. Schubert, *Chem. Commun.* **2005**, 2423–2432.
[42] O. Crespo-Biel, C. W. Lim, B. J. Ravoo, D. N. Reinhoudt, J. Huskens, *J. Am. Chem. Soc.* **2006**, *128*, 17024–17032.
[43] M. J. W. Ludden, A. Mulder, R. Tampé, D. N. Reinhoudt, J. Huskens, *Angew. Chem.* **2007**, *119*, 4182–4185; *Angew. Chem. Int. Ed.* **2007**, *46*, 4104–4107.
[44] J. D. Fikes, G. A. Barkocy-Gallagher, D. G. Klapper, P. J. Bassford, *J. Biol. Chem.* **1990**, *265*, 3417–3423.
[45] W. Boos, H. Shuman, *Microbiol. Mol. Biol. Rev.* **1998**, *62*, 204–229.
[46] L. G. Sillen, A. E. Martell, *Stability Constants of Metal-Ion Complexes. Section 2: Organic Ligands*, The Chemical Society, London, **1964**.
[47] The conditional stability constant for complex Ni•**4**, $K_{cond}=[Ni•4]/([Ni(II)][4]_{free})$, in which $[\mathbf{4}]_{free}$ represents the concentration of **4** and its protonated forms, is given by $\log K_{cond}=\log K_{Ni•4}-\log K_{H•4}+pH$ (for pH 3–10). Assuming the following values for NiNTA and HNTA, $\log K_{NiNTA}=11.5$ and $\log K_{HNTA}=9.7$, then $\log K_{cond}=9.3$ at pH 7.5.
[48] M. V. Matz, K. A. Lukyanov, S. A. Lukyanov, *BioEssays* **2002**, *24*, 953–959.
[49] N. C. Shaner, R. E. Campbell, P. A. Steinbach, B. N. G. Giepmans, A. E. Palmer, R. Y. Tsien, *Nat. Biotechnol.* **2004**, *22*, 1567–1572.
[50] V. V. Verkhusha, K. A. Lukyanov, *Nat. Biotechnol.* **2004**, *22*, 289–296.
[51] J. Wiedenmann, A. Schenk, C. Röcker, A. Girod, K. D. Spindler, G. U. Nienhaus, *Proc. Natl. Acad. Sci. U.S.A.* **2002**, *99*, 11646–11651.
[52] S. Lata, A. Reichel, R. Brock, R. Tampé, J. Piehler, *J. Am. Chem. Soc.* **2005**, *127*, 10205–10215.
[53] S. Onclin, A. Mulder, J. Huskens, B. J. Ravoo, D. N. Reinhoudt, *Langmuir* **2004**, *20*, 5460–5466.
[54] C. M. Bruinink, C. A. Nijhuis, M. Péter, B. Dordi, O. Crespo-Biel, T. Auletta, A. Mulder, H. Schönherr, G. J. Vancso, J. Huskens, D. N. Reinhoudt, *Chem. Eur. J.* **2005**, *11*, 3988–3996.
[55] P. R. Ashton, R. Königer, J. F. Stoddart, D. Alker, V. D. Harding, *J. Org. Chem.* **1996**, *61*, 903–908.

Received: September 18, 2007
Published online: January 11, 2008

  